A simple analytical model of action potential duration profile in electrotonically-coupled cells

Vincent Jacquemet[a,b]

[a] *Université de Montréal, Département de Physiologie Moléculaire et Intégrative, Montréal, Canada*
[b] *Hôpital du Sacré-Coeur de Montréal, Centre de Recherche, Montréal, Canada*

Correspondence to:

Vincent Jacquemet
Hôpital du Sacré-Coeur de Montréal
Centre de Recherche
5400 boul. Gouin Ouest
Montreal (Quebec)
Canada H4J 1C5
phone: +1 514 338 2222 ext. 2522
fax: +1 514 338 2694
vincent.jacquemet@umontreal.ca

Published in:

Math. Biosci. (2016), vol 286, vol. 272, pp. 92-99

Abstract

Electrotonic interactions between cardiac cells modulate the dispersion of action potential duration (APD). This paper provides a complete mathematical analysis of a simple model of exponential-shaped repolarization in a network of electrotonically-coupled cells with different intrinsic APDs. The forward problem consists in computing the APD map in the coupled system from the intrinsic APD map. A closed-form algebraic formula is derived for the forward problem. The inverse problem, inferring the intrinsic APDs from an APD map, is proved to have a unique solution (if any). Perturbation analysis leads to an efficient and accurate Newton-based solver for this specific inverse problem. Finally, an analytical expression is obtained for the convolution filter that

solves the forward problem in one dimension. This mathematical framework forms a solid theoretical basis for future development and validation of repolarization parameter estimation techniques in detailed models of cardiac tissue.

Keywords: computer modeling, cardiac electrophysiology, electrotonic coupling, action potential duration, parameter estimation, inverse problem

1. Introduction

The action potential duration (APD) of a cardiac cell is a commonly-used parameter to quantitatively describe cardiac cell repolarization. The intrinsic APD of a cell is the APD measured when the cell is (or if it were) isolated. When cells are coupled through gap junctions, electrotonic currents tend to reduce the differences in action potential morphology between neighboring cells. As a result, the distribution of APD observed in a tissue may significantly differ from the distribution of intrinsic APD characterizing local cellular properties [1, 2]. This is particularly true in the presence of intrinsic heterogeneities [3] and in small hearts [4, 5]. Geometry, boundary effects [6], activation pattern [7], wavefront curvature [8], wavefront collision [9], and possible coupling with fibroblasts [10, 11] also modulate APD dispersion.

Since altered dispersion of repolarization has been recognized to be arrhythmogenic [12], computer models have been developed to investigate these mechanisms. While *in vivo* experiments report APD measured in tissue or in isolated cells at a limited number of locations (e.g. biopsies), mathematical models need the spatial profile of intrinsic properties of cardiac cells as input parameters. The determination of the intrinsic APD of all the cells of a heterogeneous tissue based on the APD of the coupled cell network is a form of inverse problem. The corresponding forward problem consists in predicting the APD map of the coupled system from the intrinsic APD map. Defauw

et al. proposed a Gaussian Green's function model and a deconvolution approach to solve this problem [13].

In this paper, we explore the mathematical basis of these forward and inverse problems in a very simple model of repolarization in coupled cell network. The model is amenable to analytical calculations for both the forward and the inverse problems, and enables the study of existence and uniqueness of the solution to the inverse problem.

2. Mathematical model

2.1. Minimalist cellular model

The simplest model of repolarization is given by an exponential decay. In that model, the membrane potential u is zero at rest, instantaneously rises to 1 when the cell is stimulated above threshold (at $t = 0$), and then $u(t)$ follows the (nondimensional) equation:

$$\frac{\mathrm{d}u}{\mathrm{d}t} = -ku \ , \qquad u(0) = 1 \ , \tag{1}$$

where $k > 0$ is the only parameter of the cellular model. The shape of the resulting action potential $u(t) = \exp(-kt)$ is compared to that of a detailed atrial membrane model in Fig. 1. Although at least four state variables may be needed to replicate the morphology of a wide range of cardiac cell action potentials [14], the exponential model still reproduces the most basic feature of triangular-like atrial action potentials. Complex multi-variable models (except possibly a sum of exponentials) are unlikely to enable analytical calculations.

The action potential duration (APD), may be expressed as a function of the parameter

$$a = \frac{\int_0^{+\infty} t\, u(t)\mathrm{d}t}{\int_0^{+\infty} u(t)\mathrm{d}t} \tag{2}$$

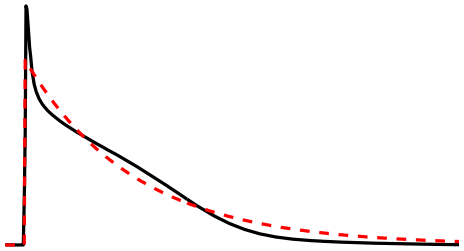

Figure 1: Action potential morphology: Nygren et al. ionic model [15] (solid line) and exponential model (red dashed line).

where the integration starts at depolarization time ($t = 0$). This quantity represents the time interval between the onset of depolarization and the center of mass of the action potential waveform. In an isolated cell with parameter k, we have $a = 1/k$, which corresponds to the time constant of the exponential, or to the APD measured at 63% repolarization. The APD might be expressed as $\gamma \cdot a$, where $\gamma \approx 2$ for a spike-and-dome action potential with steep phase 3 repolarization and $\gamma \approx 3$ for a triangular-shaped action potential. In our case of exponentially-decaying action potentials, $1/a$ represents an estimate of the apparent parameter k of a cell with action potential $u(t)$. The choice $\gamma = 3$ would correspond to an estimate of the APD at 95% repolarization. In the sequel, for the sake of simplicity, the parameter a will be referred to as APD.

This unusual choice of APD definition and the very simplified action potential shape are (probably) necessary conditions to enable the derivation of exact analytical expressions in a network of coupled cells. Section 6 illustrates how the approach can be extended to more complex models and other definitions of APD when only numerical solutions are sought.

2.2. Network of coupled cells

If n cells with parameters $k_1, \ldots, k_n$ are coupled through gap junctions, the evolution of the membrane potentials $u_1(t), \ldots, u_n(t)$ is governed by the system

$$\frac{\mathrm{d}u_i}{\mathrm{d}t} = -k_i u_i - \sum_{j=1}^{n} g_{ij}(u_i - u_j) \ , \qquad u_i(0) = 1 \ , \tag{3}$$

where $g_{ij} = g_{ji} \geq 0$ represents the coupling between cell i and cell j. The initial condition corresponds to the situation where all cells are stimulated simultaneously. This choice enables us to focus on repolarization. This equation is rewritten in matrix form

$$\frac{\mathrm{d}\mathbf{u}}{\mathrm{d}t} = -K\mathbf{u} - G\mathbf{u} \tag{4}$$

where the vector $\mathbf{u}$ contains the components u_i, the diagonal matrix K the components k_i and the symmetric semi-positive definite G the coupling conductances. The n-vector $(1, 1, \ldots, 1)$ will be denoted by $\mathbf{1}$. Using that notation, $G\mathbf{1} = \mathbf{0}$. The consequence is that ($\cdot^t$ means transposed)

$$\mathbf{1}^t \, \frac{\mathrm{d}\mathbf{u}}{\mathrm{d}t} = -\mathbf{1}^t \, K\mathbf{u} = -\mathbf{k}^t \, \mathbf{u} \ \ . \tag{5}$$

In the limit where all coupling conductances are scaled up until they uniformly tend to $+\infty$, all the u_i become identical to prevent an infinite current from flowing between the cells and the average of the membrane potentials follows the evolution of an isolated cell with $k = (k_1 + \cdots + k_n)/n$.

The evolution of the coupled system can be easily calculated using the eigenvalues $\lambda_j > 0$ and eigenvectors $\mathbf{v}_j$ of the symmetric positive definite matrix $M = K + G$

$$\mathbf{u}(t) = \exp(-Mt) \, \mathbf{1} = \sum_{j=1}^{n} \exp(-\lambda_j t) \, \mathbf{v}_j \mathbf{v}_j^t \cdot \mathbf{1} \ \ . \tag{6}$$

3. Forward problem

The purpose of this section is to provide an analytical expression for the APD of all the coupled cells, $\mathbf{a} = (a_1, \ldots, a_n)$, given their parameters $\mathbf{k} = (k_1, \ldots, k_n)$, that is, to determine the mapping $\mathbf{a} = \mathcal{A}(\mathbf{k}, G)$.

3.1. Equation for the action potential duration

After substitution of the solution (6), the numerator of (2) is given by

$$\int_0^{+\infty} t\,\mathbf{u}(t)\mathrm{d}t = \sum_{j=1}^{n} \frac{1}{\lambda_j^2}\,\mathbf{v}_j\mathbf{v}_j^t \cdot \mathbf{1} = M^{-2} \cdot \mathbf{1} \tag{7}$$

since the matrix M^{-2} has eigenvectors $\mathbf{v}_j$ with eigenvalues λ_j^{-2}. Similarly,

$$\int_0^{+\infty} \mathbf{u}(t)\mathrm{d}t = \sum_{j=1}^{n} \frac{1}{\lambda_j}\,\mathbf{v}_j\mathbf{v}_j^t \cdot \mathbf{1} = M^{-1} \cdot \mathbf{1} \quad . \tag{8}$$

If the matrix A is defined as the diagonal matrix containing the elements of $\mathbf{a}$ in its diagonal, then

$$A\,M^{-1}\,\mathbf{1} = M^{-2}\,\mathbf{1} \quad , \tag{9}$$

or, equivalently,

$$(K+G)^2\,A\,(K+G)^{-1}\,\mathbf{1} = \mathbf{1} \quad . \tag{10}$$

This equation relates, for a given distribution of coupling, the APD (A) to the intrinsic parameters (K). The vector $\mathbf{a}$ can therefore be computed by solving two linear systems instead of simulating the evolution.

In the absence of coupling ($G = 0$), $A = K^{-1}$, that is, $a_i = 1/k_i$. These values are referred to as the *intrinsic* APD.

3.2. Scaling law

It appears that the evolution equation (3) is invariant when the conductances g_{ij} are scaled by g^{-1}, the parameters k_i by g^{-1} and the time by g. As a result,

$$\mathcal{A}(\mathbf{k}, G) = g^{-1}\mathcal{A}(\mathbf{k}/g, G/g) \quad . \tag{11}$$

This enables the elimination of one parameters for explicit calculations.

3.3. Algebraic form

The vector $\mathbf{x} = (K+G)^{-1}\,\mathbf{1}$ can be obtained by solving the system $(K+G)\,\mathbf{x} = \mathbf{1}$ using Cramer's determinant-based approach. Its i-th component is expressed as a ratio of two multivariate polynomials in $k_1, \ldots, k_n$ of degree one in each of the variables, each polynomial corresponding to the expanded form of a determinant of Cramer's rule:

$$x_i = \frac{p_i(k_1, \ldots, k_n)}{q(k_1, \ldots, k_n)} \tag{12}$$

The numerator p_i does not depend on k_i and the denominator is the determinant of $K+G$. The same approach applies to $\mathbf{y} = (K+G)^{-2}\,\mathbf{1} = (K+G)^{-1}\,\mathbf{x}$ and shows that

$$y_i = \frac{r_i(k_1, \ldots, k_n)}{q(k_1, \ldots, k_n)^2} \tag{13}$$

where r_i is a multivariate polynomial of degree at most two in each of its variables. The APD is $a_i = y_i/x_i$ from (9) and is expressed as

$$a_i = \frac{r_i(k_1, \ldots, k_n)}{p_i(k_1, \ldots, k_n)\, q(k_1, \ldots, k_n)} \tag{14}$$

which is a ratio of two multivariate polynomials of degree at most two in each of its variables.

3.4. Explicit formulas

The configuration of a unidimensional chain of cells connected with a conductance g will be considered. In this case, the n-by-n tridiagonal matrix G is given by $G_{i,i+1} = G_{i,i-1} = -g$ and $G_{i,i} = 2g$ except $G_{1,1} = G_{n,n} = g$, and $G_{i,j} = 0$ otherwise.

3.4.1. Two cells

First, g is set to 1 since it can be reintroduced later using the scaling law. Following the approach of the preceding subsection,

$$M^{-1} = \begin{pmatrix} k_1+1 & -1 \\ -1 & k_2+1 \end{pmatrix}^{-1} = \frac{1}{k_1+k_2+k_1k_2} \begin{pmatrix} k_2+1 & 1 \\ 1 & k_1+1 \end{pmatrix} \tag{15}$$

which leads to

$$a_1 = \frac{k_2^2+3k_2+k_1+4}{(k_2+2)(k_1+k_2+k_1k_2)} \tag{16}$$

$$a_2 = \frac{k_1^2+3k_1+k_2+4}{(k_1+2)(k_1+k_2+k_1k_2)} \tag{17}$$

In the particular case $k_1 = k_2$, as expected, $a_1 = a_2 = 1/k_1$. In the presence of coupling g, the scaling formula (11) becomes

$$a_1 = \frac{k_2^2/g^2+3k_2/g+k_1/g+4}{(k_2/g+2)(k_1+k_2+k_1k_2/g)} \tag{18}$$

Note that in the two limit cases

$$\lim_{g\to\infty} a_1 = \frac{2}{k_1+k_2} \qquad \text{and} \qquad \lim_{g\to 0} a_1 = \frac{1}{k_1} \tag{19}$$

which means that without coupling the situation is the same as isolated cells and when the coupling becomes very large both cells have the same APD associated with the arithmetic mean of the parameter k_1 and k_2, as expected from (5).

3.4.2. Three cells

To solve the equation for $n = 3$ and more, symbolic calculation software was used (Mathematica 10.1). The APD for $g = 1$ are given by the following algebraic expressions:

$$a_1 = \frac{\begin{pmatrix} k_1k_2 + k_1k_3^2 + 3k_1k_3 + 5k_1 + k_2^2k_3^2 + 2k_2^2k_3 + k_2^2 + 5k_2k_3^2 + 9k_2k_3 \\ +5k_2 + 8k_3^2 + 14k_3 + 9 \end{pmatrix}}{(k_2k_3 + k_2 + 3k_3 + 3)(k_1k_2k_3 + k_1k_2 + 2k_1k_3 + k_1 + k_2k_3 + k_2 + k_3)} \tag{20}$$

$$a_2 = \frac{\begin{pmatrix} k_1^2k_2 + k_1^2k_3^2 + 3k_1^2k_3 + 5k_1^2 + 2k_1k_2 + 3k_1k_3^2 + 8k_1k_3 + 11k_1 \\ +k_2k_3^2 + 2k_2k_3 + 2k_2 + 5k_3^2 + 11k_3 + 9 \end{pmatrix}}{(k_1k_3 + 2k_1 + 2k_3 + 3)(k_1k_2k_3 + k_1k_2 + 2k_1k_3 + k_1 + k_2k_3 + k_2 + k_3)} \tag{21}$$

$$a_3 = \frac{\begin{pmatrix} k_1^2k_2^2 + 5k_1^2k_2 + k_1^2k_3 + 8k_1^2 + 2k_1k_2^2 \\ +9k_1k_2 + 3k_1k_3 + 14k_1 + k_2^2 + k_2k_3 + 5k_2 + 5k_3 + 9 \end{pmatrix}}{(k_1k_2 + 3k_1 + k_2 + 3)(k_1k_2k_3 + k_1k_2 + 2k_1k_3 + k_1 + k_2k_3 + k_2 + k_3)} \tag{22}$$

After scaling by the conductance parameter, the limit cases are

$$\lim_{g\to\infty} a_1 = \frac{3}{k_1 + k_2 + k_3} \qquad \text{and} \qquad \lim_{g\to 0} a_1 = \frac{1}{k_1} \quad . \tag{23}$$

4. Inverse problem

The inverse problem consists in finding parameters $\mathbf{k}$ such that the APD profile $\mathbf{a}$ reproduces a desired target APD profile. This means inverting the mapping $\mathcal{A}$ to compute the mapping $\mathbf{k} = \mathcal{A}^{-1}(\mathbf{a}, G)$.

4.1. Existence and uniqueness of the solution

4.1.1. Two cells

In the case $n = 2$, the difference in APD between the two cells is given by

$$a_2 - a_1 = \frac{k_1 - k_2}{(k_1 + 2)(k_2 + 2)} \tag{24}$$

and is clearly bounded since

$$\sup_{k_1>0,\ k_2>0} |a_2 - a_1| = \lim_{k_1\to+\infty} \lim_{k_2\to 0} |a_2 - a_1| = \frac{1}{2} \quad . \tag{25}$$

After reintroduction of the conductance by scaling, this means that the inverse problem has no solution when $|a_2 - a_1| > 1/2g$. This condition fixes a limit on the APD gradient that can be observed in two coupled cells and is more restrictive when the coupling is large.

Although the solution may not exist for all (a_1, a_2), when it exists, it is unique. The Jacobian of $-\mathcal{A}(k_1, k_2)$

$$-D\mathcal{A} = \begin{pmatrix} \frac{k_2^2+2k_2+2}{(k_2k_1+k_1+k_2)^2} & \frac{(2k_2+3)k_1^2+(6k_2+8)k_1+k_2^2+8k_2+8}{(k_2+2)^2(k_2k_1+k_1+k_2)^2} \\ \frac{k_1^2+2\left(k_2^2+3k_2+4\right)k_1+3k_2^2+8k_2+8}{(k_1+2)^2(k_2k_1+k_1+k_2)^2} & \frac{k_1^2+2k_1+2}{(k_2k_1+k_1+k_2)^2} \end{pmatrix} \tag{26}$$

has only positive entries for all $k_1 > 0$, $k_2 > 0$. Moreover, its determinant

$$\det(-D\mathcal{A}) = \frac{k_1^2\left(k_2^2+4k_2+5\right)+2k_1\left(2k_2^2+7k_2+8\right)+5k_2^2+16k_2+16}{(k_1+2)^2(k_2+2)^2(k_1k_2+k_1+k_2)^2} \tag{27}$$

is also always positive. This implies that $-D\mathcal{A}$ is a P-matrix. Note that these conditions would not be satisfied if a negative coupling $g < 0$ was used. The application of the Gale–Nikaido theorem (see next paragraph) shows that $\mathcal{A}$ is injective, so the inverse problem has at most one solution. Analytical solutions for $n = 2$ and $n = 3$ will be presented below.

4.1.2. The Gale–Nikaido theorem

A P-matrix is a square matrix whose principal minors are all positive. The Gale–Nikaido theorem [16] states that if a differentiable mapping from a closed rectangular region $\Omega \subset \mathbb{R}^n$ to $\mathbb{R}^n$ is such that its Jacobian is a P-matrix for every point in Ω, then the mapping is injective. This means that there is a global inverse mapping, and

not only a local one guaranteed by the implicit function theorem when the Jacobian is non-singular.

In our case, the rectangular region is $\mathbb{R}^n_+$, and since increasing the parameter k decreases the APD, the minors are expected to be negative so the theorem has to be applied to $-\mathcal{A}$ as in the case $n = 2$ seen above.

Gale and Nikaido proposed a geometric characterization of P-matrices that leads to a simple physiological interpretation [16]. A matrix M is said to *reverse the sign* of a vector $\mathbf{x}$ if $x_i \cdot (M\mathbf{x})_i \leq 0$ for all i, where $(M\mathbf{x})_i$ stands for the i-th component of $M\mathbf{x}$. Then, the matrix M is a P-matrix if and only if M reverses the sign of no vector other than the null vector.

In the context of a network of cells, the Jacobian describes the change in APD in the coupled system resulting from a change in the parameters of the cells. The P-matrix condition stipulates that although a cell might have a prolonged APD despite a reduced intrinsic APD or a shortened APD despite an increased intrinsic APD (due to the coupling with its neighbors), this sort of "opposite reaction" effect can never occur in *all* the cells at the same time. In a diffusive system, this condition seems physiologically reasonable.

4.1.3. General case

To compute the Jacobian of $\mathcal{A}$, a perturbation approach will be applied to the implicit relation (10). A perturbation of $K = K_0 + \epsilon K_1$ results in a change in $A = A_0 + \epsilon A_1$, where $\epsilon \ll 1$ and all those matrices are diagonal. Then, $M = M_0 + \epsilon K_1$ with $M_0 = K_0 + G$. Up to first order in ϵ,

$$M^2 = M_0^2 + \epsilon \, (M_0 K_1 + K_1 M_0) \tag{28}$$

$$M^{-1} = M_0^{-1} - \epsilon \, M_0^{-1} K_1 M_0^{-1} \tag{29}$$

After insertion in (10), the identification of zero-th and first-order terms in ϵ gives $M_0^2 A_0 M_0^{-1}\mathbf{1} = \mathbf{1}$ and

$$\left((M_0K_1 + K_1M_0)A_0M_0^{-1} + M_0^2A_1M_0^{-1} - M_0^2A_0M_0^{-1}K_1M_0^{-1}\right)\mathbf{1} = \mathbf{0} \tag{30}$$

The matrix A_1 is then isolated. With the notation $\mathbf{x}_0 = M_0^{-1}\mathbf{1}$,

$$A_1\mathbf{x}_0 = A_0M_0^{-1}K_1\mathbf{x}_0 - M_0^{-2}(M_0K_1 + K_1M_0)A_0\mathbf{x}_0 \quad . \tag{31}$$

This equation provides a linear relation between $\mathbf{k}_1 = K_1\mathbf{1}$ and $\mathbf{a}_1 = A_1\mathbf{1}$ that is identified with the definition of the Jacobian $\mathbf{a}_1 = D\mathcal{A}\cdot\mathbf{k}_1$.

To prove by contradiction that $-D\mathcal{A}$ is a P-matrix, let us assume that there exists a non-null vector $\mathbf{k}_1$ such that $-D\mathcal{A}$ reverses the sign of $\mathbf{k}_1$. This means that all the components of the vector $K_1(-A_1)\mathbf{1}$ are ≤ 0 since $-(D\mathcal{A})(\mathbf{k}_1) = -A_1\mathbf{1}$. From (8), all the components of $\mathbf{x}_0$ are positive, so the previous condition implies that

$$\mathbf{x}_0^tK_1A_1\mathbf{x}_0 \geq 0 \quad . \tag{32}$$

Using (31), the inequality becomes

$$\mathbf{x}_0^tK_1\left(A_0M_0^{-1}K_1 - M_0^{-1}K_1A_0 - M_0^{-2}K_1M_0A_0\right)\mathbf{x}_0 \geq 0 \quad . \tag{33}$$

To simplify the third term, note that

$$M_0A_0\mathbf{x}_0 = M_0^{-1}M_0^2A_0M_0^{-1}\mathbf{1} = M_0^{-1}\mathbf{1} = \mathbf{x}_0 \quad , \tag{34}$$

which leads to

$$(K_1\mathbf{x}_0)^t\left(A_0M_0^{-1} - M_0^{-1}A_0 - M_0^{-2}\right)(K_1\mathbf{x}_0) \geq 0 \quad . \tag{35}$$

Since the sum of the first two terms is antisymmetric and M_0^{-2} is symmetric positive definite, then necessarily $K_1\mathbf{x}_0 = \mathbf{0}$, which implies $\mathbf{k}_1 = \mathbf{0}$ because the components of $\mathbf{x}_0$ are all positive. This shows that the Jacobian is a P-matrix and therefore that the mapping $\mathcal{A}$ is injective in the general case. Note that the fact that G (and thus M_0^{-2}) is symmetric semi-positive definite was critical in the proof.

4.2. Explicit formulas

With the help of Mathematica, exact closed-form formulas were found for the inverse problem $\mathcal{A}^{-1}(\mathbf{a})$, which enabled us to determine the domain of the function $\mathcal{A}^{-1}$. These domains can be represented graphically for $n = 2$ and $n = 3$.

4.2.1. Two cells

The inverse of relations (16) and (17) is given by the algebraic expressions:

$$k_1 = \frac{2a_2^2 - 2a_1a_2 - a_1 + a_2 + 1}{a_1a_2 + a_1 - a_2^2} \tag{36}$$

$$k_2 = \frac{2a_1^2 - 2a_1a_2 + a_1 - a_2 - 1}{a_1a_2 + a_2 - a_1^2} \quad . \tag{37}$$

The domain in which the conditions $k_1 > 0$ and $k_2 > 0$ are satisfied is shown in Fig. 2.

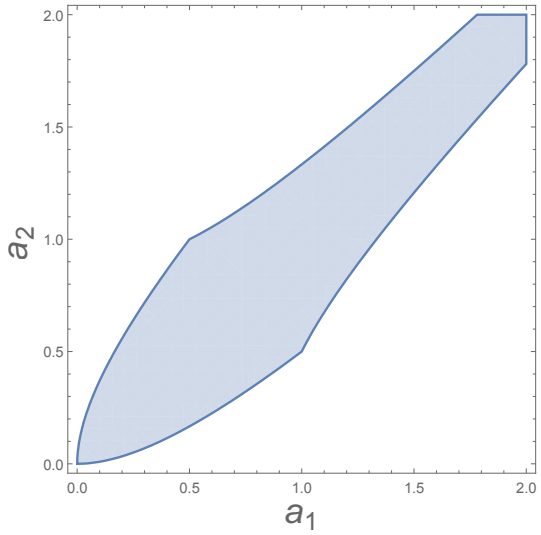

Figure 2: Domain of the (a_1, a_2) plane in which the inverse problem has a unique solution in the case of two coupled cells.

4.2.2. Three cells

For $n = 3$, the solution of the inverse problem reads:

$$k_1 = \frac{-a_1a_2^2+a_1a_2a_3-2a_1a_2-a_1+a_2^2a_3+3a_2^2-a_2a_3^2-a_2a_3+a_2+1}{a_1a_2^2-a_1a_2a_3+a_1a_2+a_1-a_2^2a_3-a_2^2+a_2a_3^2} \tag{38}$$

$$k_2 = \frac{-a_1^2a_2-3a_1^2+2a_1a_2a_3+3a_1a_2-a_1-a_2a_3^2+3a_2a_3+2a_2-3a_3^2-a_3-1}{a_1^2-a_1a_2-a_2a_3-a_2+a_3^2} \tag{39}$$

$$k_3 = \frac{a_1^2a_2-a_1a_2^2-a_1a_2a_3+a_1a_2+a_2^2a_3-3a_2^2+2a_2a_3-a_2+a_3-1}{-a_1^2a_2+a_1a_2^2+a_1a_2a_3-a_2^2a_3+a_2^2-a_2a_3-a_3} \tag{40}$$

The domain in which the conditions $k_1 > 0$, $k_2 > 0$ and $k_3 > 0$ are satisfied is shown in Fig. 3. The domain is symmetric with respect to permutation of a_1 and a_3, but a_2 plays a slightly different role since it represents the APD of the cell in the middle.

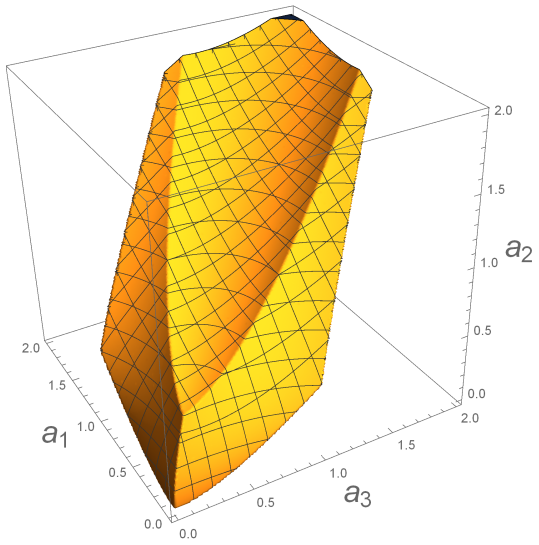

Figure 3: Domain of the (a_1, a_2, a_3) space in which the inverse problem has a unique solution in the case of a chain of three coupled cells.

4.3. Numerical solution

To numerically solve the inverse problem, we are going to use a Newton-based approach. The APD profile in the coupled system (A) is supposed to be known and

we seek a set of parameters (K) that satisfies (10). A first approximation is obtained from $K_0 = A^{-1}$, assuming $G = 0$ as a first step. Then a linear approximation around $K = K_0$ will enable us to iteratively refine the solution.

To derive the update formula, we set $K = K_0 + \epsilon K_1$, where ϵ is small parameter that will eventually be set to 1. The matrix A, however, is known so it does not have a perturbation term. Using the notations of paragraph 4.1.3, equation (10) is written as

$$\left(M_0^2 A M_0^{-1} + \epsilon \left((M_0 K_1 + K_1 M_0) A M_0^{-1} - M_0^2 A M_0^{-1} K_1 M_0^{-1}\right)\right) \mathbf{1} = \mathbf{1} \tag{41}$$

up to first order in ϵ. Then, we set $\epsilon = 1$ and $M_0^{-1}\mathbf{1} = \mathbf{x}_0$, and the equation becomes

$$M_0 K_1 A \mathbf{x}_0 + K_1 M_0 A \mathbf{x}_0 - M_0^2 A M_0^{-1} K_1 \mathbf{x}_0 = \mathbf{1} - M_0^2 A \mathbf{x}_0 \ . \tag{42}$$

This is a linear equation for the correction term K_1. To make it more explicit for programming purpose, the definition $\mathbf{k}_1 = K_1\mathbf{1}$ and the notation $\mathrm{diag}(\mathbf{k}_1) = K_1$ for diagonal matrices are used. Noting that for any vector $\mathbf{v}$, $K_1\mathbf{v} = \mathrm{diag}(\mathbf{v}) \cdot \mathbf{k}_1$, the linear system in $\mathbf{k}_1$ is

$$\left(M_0 \mathrm{diag}(A\mathbf{x}_0) + \mathrm{diag}(M_0 A \mathbf{x}_0) - M_0^2 A M_0^{-1} \mathrm{diag}(\mathbf{x}_0)\right) \mathbf{k}_1 = \mathbf{1} - M_0^2 A \mathbf{x}_0 \ . \tag{43}$$

The algorithm works as follows. The inputs are A and G. The initial estimate for the parameter vector $\mathbf{k}$ is given by $\mathbf{k}^{(0)} = A^{-1}\mathbf{1}$. Then, at iteration i, M_0 and $\mathbf{x}_0$ are updated based on $\mathbf{k}^{(i-1)}$, the linear system (43) is solved and its solution $\Delta\mathbf{k}$ is used to refine the estimate $\mathbf{k}^{(i)} = \mathbf{k}^{(i-1)} + \Delta\mathbf{k}$. The iterations stop when $\|\Delta\mathbf{k}\|_\infty < tol$, i.e. when the maximal error falls below a tolerance value.

Figure 4 provides examples of convergence of the inverse problem algorithm. In all cases, including randomly distributed intrinsic APD values where the APD profile significantly differs from the intrinsic APD, the maximal error becomes $< 10^{-8}$ after 3 iterations only, both in a uniform cable (left panels) and in a cable with an abrupt

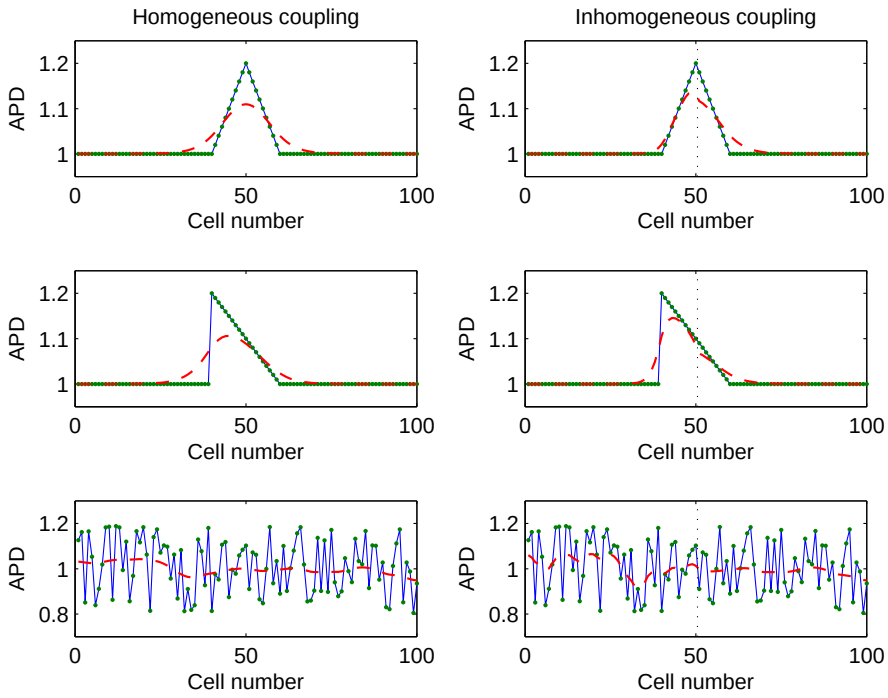

Figure 4: Illustration of the convergence of the inverse problem solver in a cable ($n = 100$). In each panel, the blue solid line represents the intrinsic action potential duration (APD, in arbitrary unit), the red dashed line is the APD profile in the coupled system and the green dots are the intrinsic APD estimated by solving the inverse problem. In the left panels, the cable is uniform ($g = 10$). In the right panels, the left half of the cable has $g = 2$ and the right half $g = 10$. The abrupt transition in conductance is indicated by the vertical dotted line.

change in conduction properties (right panels). Note that in the inhomogeneous case, the APD profile follows more closely the intrinsic APD on the left half of the cable associated with weaker coupling.

5. Near-uniform tissue properties

Although the domain of the function $\mathcal{A}^{-1}(\mathbf{a})$ might be complex in the general case, it will necessarily include the diagonal line $a_1 = a_2 = \cdots = a_n$ and its vicinity. Per-

turbation analysis around the diagonal line will enable us to express the APD as a convolution of the intrinsic APD and a kernel function.

5.1. Perturbation analysis

We start with (31) applied to the particular case where A_0 and K_0 are proportional to the identity matrix I, i.e. $A_0 = a_0 I$, which means that $A_0 = K_0^{-1}$. This is a consequence of the simultaneous activation of the tissue. During impulse propagation in a tissue with uniform properties, the APD would not be uniform near tissue boundary.

The fact that the two matrices A_0 and K_0 commute with *all* matrices, combined with the relation $G\mathbf{1} = \mathbf{0}$, implies that $(M_0)^m\mathbf{1} = (K_0)^m\mathbf{1}$ for any integer m, and in particular $\mathbf{x}_0 = M_0^{-1}\mathbf{1} = K_0^{-1}\mathbf{1}$. In this context, (31) becomes

$$A_1 K_0^{-1}\mathbf{1} = A_0 M_0^{-1} K_1 K_0^{-1}\mathbf{1} - M_0^{-2}(M_0 K_1 + K_1 M_0) A_0 K_0^{-1}\mathbf{1} \quad . \tag{44}$$

The first and second term (after expansion) of the right hand side cancel each other, so the equation is simplified to

$$A_1\mathbf{1} = -A_0 M_0^{-2} K_1 M_0\mathbf{1} = -M_0^{-2} K_1\mathbf{1} \quad , \tag{45}$$

where we used $M_0\mathbf{1} = A_0^{-1}\mathbf{1}$.

The intrinsic APD, represented by the diagonal matrix A_i, is given by

$$A_i = K^{-1} = (K_0 + \epsilon K_1)^{-1} = A_0 - \epsilon A_0^2 K_1 \tag{46}$$

at first order in ϵ. By combining (45) and (46),

$$M_0^{-2} A_i\mathbf{1} = A_0 M_0^{-2}\mathbf{1} - \epsilon A_0^2 M_0^{-2} K_1\mathbf{1} = A_0 K_0^{-2}\mathbf{1} + \epsilon A_0^2 A_1\mathbf{1} \tag{47}$$

which finally leads to the relation

$$A\,\mathbf{1} = A_0^{-2} M_0^{-2} A_i\mathbf{1} = (I + A_0 G)^{-2} A_i\mathbf{1} \tag{48}$$

describing the filter that transforms the intrinsic APD profile into the APD profile in the coupled cell network.

5.2. Solution in a ring

If the cell network configuration is a ring of n cells connected to their two neighbors by a conductance g, the discrete Fourier transform matrix F diagonalizes the matrix G, i.e.,

$$G\,F = \Lambda\,F \quad , \tag{49}$$

where the diagonal matrix Λ has values Λ_j on its diagonal [17]

$$\Lambda_j = 4g\sin^2\frac{(j-1)\pi}{n} \quad . \tag{50}$$

As a result, the transfer function of the filter $A_0^{-2}M_0^{-2}$ of (48) is

$$H_d(\omega,\kappa) = \frac{1}{\left(1+\kappa\sin^2(\omega)\right)^2} \tag{51}$$

where $\kappa = 4a_0g$ and d stands for discrete. In other words, the APD profile is obtained by computing the discrete Fourier transform of the intrinsic APD profile, by multiplying the j-th component by $H_d((j-1)\pi/n),\kappa)$ for all j, and by taking the inverse discrete Fourier transform.

5.3. Continuum limit

Consider a uniform ring of length L. The discretization of the cable equation with conductivity σ into n elements leads to the discrete system studied in the previous paragraph with $g = n^2\sigma/L^2$. The continuum limit therefore corresponds to $n \to +\infty$ and $g \to +\infty$ with the constraint $n^2/g = L^2/\sigma =$ constant. In the continuous ring, the fundamental frequency is $\omega_0 = 2\pi/L$. A_i and A are now decomposed in Fourier series. Through the application of the filter, the j-th term of the series is multiplied by (j now starts at 0)

$$\begin{aligned} H_j &= \lim_{n\to\infty} H_d\left(j\pi/n, 4a_0n^2\sigma/L^2\right) = \lim_{n\to\infty}\left(1+4a_0\frac{n^2\sigma}{L^2}\sin^2\frac{j\pi}{n}\right)^{-2} \\ &= \left(1+a_0\sigma\omega_0^2j^2\right)^{-2} \quad . \end{aligned} \tag{52}$$

In order to obtain the solution in an infinite cable, the limit $L \to +\infty$ is calculated. In this case, the Fourier series will be replaced by a Fourier transform. The transfer function in the Fourier domain is given by function $H_c(\omega)$, where c stands for continuous, such that $H_c(j\omega_0) = H_j$. If $L \to +\infty$, then $\omega_0 \to 0$ and the transfer function is given by

$$H_c(\omega) = \frac{1}{\left(1 + a_0\sigma\omega^2\right)^2} \quad . \tag{53}$$

The inverse Fourier transform of $H_c(\omega)$ provides a spatial representation of the convolution filter

$$h_c(x) = \frac{|x| + \sqrt{a_0\sigma}}{4a_0\sigma} \exp\left(-\frac{|x|}{\sqrt{a_0\sigma}}\right) \quad . \tag{54}$$

Note that $h_c'(0) = 0$ and $\int_{-\infty}^{+\infty} h_c(x)\mathrm{d}x = 1$.

Figure 5 compares APD profiles obtained using the exact formula (10), the linear perturbation approach (48) and the convolution formula (54). The tissue properties reproduce the situation of the impulse response of a filter, that is, a single cell in the middle of the cable has an intrinsic APD increased by a factor $1 + \epsilon$. Provided that the cable is long enough, the linear perturbation and the convolution give the same result (dots vs dotted line). As ϵ is increased to 0.2, the non-linearity of the relation between k an a becomes non-negligible and some discrepancies are observed near the high gradient of intrinsic APD (solid line vs dots).

6. Possible extensions

The inverse solver presented here is very efficient but heavily relies on the formulation of the simplified cell model and the particular choice of APD definition. In this section, a proof-of-concept example is provided to give some insights into how these assumptions may be alleviated to solve practical problems.

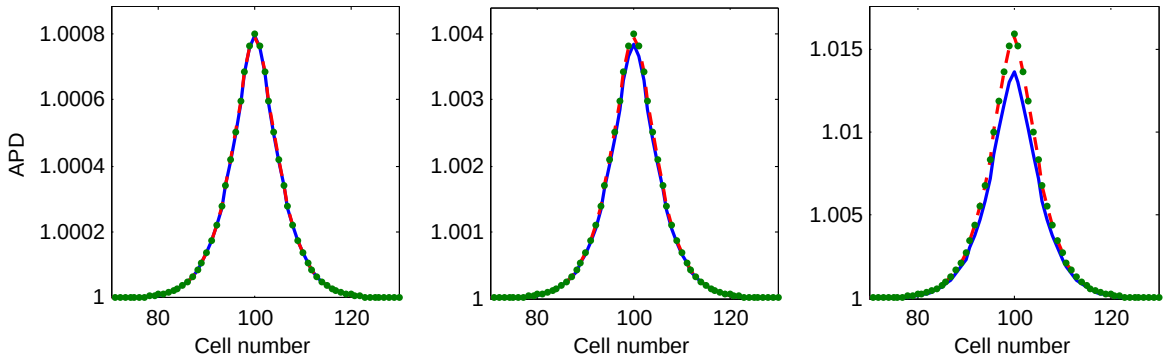

Figure 5: Action potential duration (APD) profile in a ring of $n = 200$ cells with coupling $g = 10$. The intrinsic APD is set to 1 except at cell 100 where it is set to $1 + \epsilon$. Left panel: $\epsilon = 0.01$; middle panel $\epsilon = 0.05$; right panel: $\epsilon = 0.2$. The solid blue curves represent the exact profiles (arbitrary unit) computed using (10). The green dots represent the local approximation ($\epsilon \ll 1$) obtained from (48), and the red dashed line the convolution with the kernel (54).

The tissue configuration is inspired from canine models of atrial tissue with inhomogeneous distribution of acetylcholine (ACh) [18, 19]. Membrane kinetics is described by a detailed model including an ACh-dependent K^+ channel [18]. A 2-cm cable with 200 cells and a conductivity of 4 mS/cm is considered. ACh plays the role of the parameter k and varies along the cable. The vector $\mathbf{k}$ is constructed from the ACh values of all 200 cells.

The forward problem is numerically solved by simulating the evolution of the tissue using the monodomain equation combined with finite difference methods. After simultaneous stimulation of the whole tissue, the duration of the resulting action potentials are measured at a threshold of -70 mV. This enables us to compute the APD profile $\mathbf{a}$ as a function of the ACh profile $\mathbf{k}$

$$\mathbf{a} = \mathbf{a}_{\text{forw}}(\mathbf{k}) \ . \tag{55}$$

The target APD profile $\mathbf{a}_{\text{target}}$ is constructed from a predefined sigmoid ACh profile

$\mathbf{k}_{\text{target}}$ (Fig. 6, bottom panel) using the formula $\mathbf{a}_{\text{target}} = \mathbf{a}_{\text{forw}}(\mathbf{k}_{\text{target}})$.

The simplest solver for the inverse problem can be described as follows. The ACh profile is first initialized: $\mathbf{k}_0 = \mathbf{0}$. Then, at iteration i, the ACh profile is updated using the formula

$$\mathbf{k}_{i+1} = \mathbf{k}_i + \mu \cdot (\mathbf{a}_{\text{forw}}(\mathbf{k}_i) - \mathbf{a}_{\text{target}}) \tag{56}$$

where μ is a constant. The iteration process stops when the error $\|\mathbf{a}_{\text{forw}}(\mathbf{k}_i) - \mathbf{a}_{\text{target}}\|$ falls below a tolerance.

Figure 6 shows the resulting APD and ACh profiles after 5 and 50 iterations using $\mu = 0.04$. These preliminary results suggest that the principles presented in this paper may be generalized to develop inverse solvers for a wider range of models. Refinements of the algorithm will certainly improve performance.

7. Discussion and conclusion

This paper presents a model of cardiac cell repolarization in a network of coupled cells. The mathematical formulation is sufficiently simple to be amenable to analytical calculations. The simplest action potential shape (exponential decrease in membrane potential) is assumed and all cells are supposed to be activated simultaneously. Another point that has been ignored is the beat-to-beat variations in APD or heart rate dependence in APD. As a result of these simplifying hypotheses, exact, closed form relations are obtained for both the forward and the inverse problem.

An interesting questions is how far the results of this simple model may be generalized to more detailed, physiologically realistic model of cardiac cells. First, the forward problem can be easily simulated in a tissue with any cardiac cell model. The choice of a single parameter to describe repolarization may need to be adjusted to each application, e.g. the conductance of the slow outward K^+ current [13]. Note that the derivations

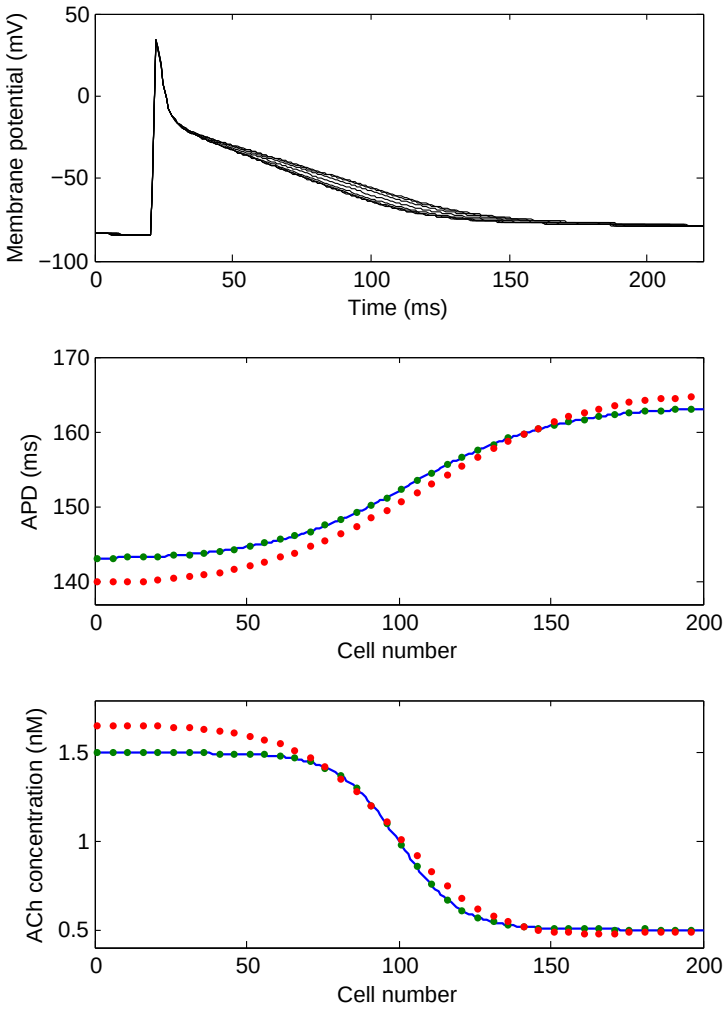

Figure 6: Example of inverse problem solving using an ionic-based membrane model. Top panel: Action potentials with ACh concentration varying from 0.5 to 1.5 nM. Middle panel: Target APD distribution (blue solid line), estimated APD distribution after 5 iterations (red dots), and estimated APD distribution after 50 iterations (green dots). Bottom panel: Target ACh profile (blue solid line), estimated ACh profile after 5 iterations (red dots), and estimated ACh profile after 50 iterations (green dots).

in this paper implicitly assume a monotonic relation between the parameter and APD. This is often the case, at least over the interval of interest. The definition of APD may also be different. We chose the definition that is amenable to analytical formulas, but many studies use a threshold at 90% repolarization. The site of stimulation matters; the APD profile is slightly different depending on the direction of propagation. It is therefore desirable to consider the situation of simultaneous activation, which can be obtained by stimulating all the tissue at the same time. When a natural activation pattern is expected (e.g. sinus rhythm), the APD profile may be computed during normal propagation instead of simultaneous activation to facilitate comparison with experimental data. Novel propagation equations based on fractional diffusion have been proposed, with potential impact on repolarization dispersion [20]. Since our formulation is based on a general discrete coupling matrix G, the approach remains applicable as long as coupling is represented by a linear self-adjoint operator that can be discretized into a matrix form (possibly non-sparse due to non-locality).

The proof of existence and uniqueness of the inverse problem is a major finding of this paper. The Gale–Nikaido condition for P-matrices (paragraph 4.1.2) is physiologically reasonable so it is plausible that the uniqueness extends to more complex models. The proposed algorithm to solve the inverse problem has perfect convergence and accuracy performances, but is very specific to our exponential model and relies heavily on the availability of an exact analytical expression for the Jacobian of the forward problem. Note also that since the forward problem maps $\mathbb{R}_+^n$ to a restricted domain around the diagonal line (see Fig. 3), the inverse problem is expected to amplify uncertainties on target APD values and may be sensitive to errors in the forward problem (here the forward problem is solved exactly). Another computational limitation is that the linear system (43) is not sparse. Thus, new algorithms will be needed to solve more general problems. Section 6 provides some guidance for future developments.

An insightful result of this simple model is the kernel function derived in the context of local linear approximation of the forward problem, assuming uniform coupling. While previous studies have used a Gaussian function [13, 21], our function is more peaked at the center and has slower decay at large distance. It remains to be seen whether our function outperforms the Gaussian in more realistic tissue models and how much this function depends on our choice of APD definition.

In conclusion, our complete analysis of a simple model forms a solid theoretical basis for future development and validation of algorithms for estimating the intrinsic membrane parameters that give rise to observed APD distribution patterns.

Conflict of interest statement

None declared.

Acknowledgments

This work was supported by the Natural Sciences and Engineering Research Council of Canada (NSERC grant RGPIN-2015-05658).

References

[1] R. Joyner, Modulation of repolarization by electrotonic interactions., Japanese heart journal 27 (1986) 167–183.

[2] M. D. Lesh, M. Pring, J. F. Spear, Cellular uncoupling can unmask dispersion of action potential duration in ventricular myocardium. A computer modeling study., Circulation Research 65 (5) (1989) 1426–1440.

[3] P. C. Franzone, L. Pavarino, B. Taccardi, Effects of transmural electrical heterogeneities and electrotonic interactions on the dispersion of cardiac repolarization and action potential duration: A simulation study, Mathematical biosciences 204 (1) (2006) 132–165.

[4] K. J. Sampson, C. S. Henriquez, Electrotonic influences on action potential duration dispersion in small hearts: a simulation study, American Journal of Physiology-Heart and Circulatory Physiology 289 (1) (2005) H350–H360.

[5] R. D. Walton, O. Bernus, Electrotonic effects on action potential duration in perfused rat hearts, in: Engineering in Medicine and Biology Society, 2009. EMBC 2009. Annual International Conference of the IEEE, IEEE, 2009, pp. 4190–4193.

[6] E. M. Cherry, F. H. Fenton, Effects of boundaries and geometry on the spatial distribution of action potential duration in cardiac tissue, Journal of theoretical biology 285 (1) (2011) 164–176.

[7] R. C. Myles, O. Bernus, F. L. Burton, S. M. Cobbe, G. L. Smith, Effect of activation sequence on transmural patterns of repolarization and action potential duration in rabbit ventricular myocardium, American Journal of Physiology-Heart and Circulatory Physiology 299 (6) (2010) H1812–H1822.

[8] P. Comtois, A. Vinet, Curvature effects on activation speed and repolarization in an ionic model of cardiac myocytes, Physical Review E 60 (4) (1999) 4619.

[9] B. M. Steinhaus, K. W. Spitzer, S. Isomura, Action potential collision in heart tissue-computer simulations and tissue experiments, Biomedical Engineering, IEEE Transactions on (10) (1985) 731–742.

[10] K. A. MacCannell, H. Bazzazi, L. Chilton, Y. Shibukawa, R. B. Clark, W. R. Giles, A mathematical model of electrotonic interactions between ventricular myocytes and fibroblasts, Biophysical journal 92 (11) (2007) 4121–4132.

[11] V. Jacquemet, C. S. Henriquez, Loading effect of fibroblast-myocyte coupling on resting potential, impulse propagation, and repolarization: insights from a microstructure model, American Journal of Physiology-Heart and Circulatory Physiology 294 (5) (2008) H2040–H2052.

[12] M. J. Killeen, I. N. Sabir, A. A. Grace, C. L.-H. Huang, Dispersions of repolarization and ventricular arrhythmogenesis: Lessons from animal models, Progress in biophysics and molecular biology 98 (2) (2008) 219–229.

[13] A. Defauw, I. V. Kazbanov, H. Dierckx, P. Dawyndt, A. V. Panfilov, Action potential duration heterogeneity of cardiac tissue can be evaluated from cell properties using Gaussian Green's function approach, PLoS ONE 8 (11) (2013) e79607.

[14] A. Bueno-Orovio, E. M. Cherry, F. H. Fenton, Minimal model for human ventricular action potentials in tissue, Journal of theoretical biology 253 (3) (2008) 544–560.

[15] A. Nygren, C. Fiset, L. Firek, J. Clark, D. Lindblad, R. Clark, W. Giles, Mathematical model of an adult human atrial cell the role of K+ currents in repolarization, Circulation Research 82 (1) (1998) 63–81.

[16] D. Gale, H. Nikaido, The Jacobian matrix and global univalence of mappings, Math. Annalen 159 (1965) 81–93.

[17] J. C. Strikwerda, Finite Difference Schemes and Partial Differential Equations, 2nd Edition, SIAM, Philadelphia, PA, 2004.

[18] J. Kneller, R. Zou, E. J. Vigmond, Z. Wang, L. J. Leon, S. Nattel, Cholinergic atrial fibrillation in a computer model of a two-dimensional sheet of canine atrial cells with realistic ionic properties, Circulation research 90 (9) (2002) e73–e87.

[19] E. Matene, A. Vinet, V. Jacquemet, Dynamics of atrial arrhythmias modulated by time-dependent acetylcholine concentration: a simulation study, Europace 16 (suppl 4) (2014) iv11–iv20.

[20] A. Bueno-Orovio, D. Kay, V. Grau, B. Rodriguez, K. Burrage, Fractional diffusion models of cardiac electrical propagation: role of structural heterogeneity in dispersion of repolarization, Journal of The Royal Society Interface 11 (97) (2014) 20140352.

[21] P. Comtois, A. Vinet, Stability and bifurcation in an integral-delay model of cardiac reentry including spatial coupling in repolarization, Physical Review E 68 (5) (2003) 051903.